

## NUMERICAL MODELLING OF FREE THIN FILM DYNAMICS

L. POPOVA<sup>1</sup>, G. GROMYKO<sup>2</sup> and S. TABAKOVA<sup>3</sup>

<sup>1</sup>*Department of Applied Mathematics and Modeling, University of Plovdiv*  
24, Tzar Asen, str., 4000 Plovdiv, Bulgaria

E-mail: lubpop@ulcc.pu.acad.bg

<sup>2</sup>*Institute of Mathematics of National Academy of Sciences of Belarus*  
Surganov 11, 220072, Minsk, Belarus

E-mail: grom@im.bas-net.by

<sup>3</sup>*Department of Mechanics, Technical University - Plovdiv*  
61 Sankt Peterburg, blvd., 4000 Plovdiv, Bulgaria

E-mail: stabakova@hotmail.com

Received September 29, 2002

### ABSTRACT

The dynamics of a free thin film attached to a rectangular frame surrounded by an ambient gas is studied theoretically. The mathematical model is described by evolutionary nonlinear system for the longitudinal velocity components and film thickness. The 1D form of the nonstationary problem is solved by a finite difference scheme. The film shape evolution in time is tracked at different Reynolds numbers,  $Re$ . The steady state solutions are reached asymptotically in time for a large range of  $Re$ .

**Key words:** finite-difference method, modelling, nonlinear system, free thin film

### 1. INTRODUCTION

The problems of thin film dynamics are of great importance for a variety of technological processes including liquid-liquid or liquid-gas disperse systems: emulsions, foams, coalescence of drops, thin film layer coatings, etc. The free thin films can be observed as attached on a thin frame when pulling the frame from a liquid in a vessel; between two deformed drops or bubbles during their coalescence. It is experimentally established that the coalescence

of these particles [2] is preceded by their initial approach, subsequent thinning (drainage) of the liquid layer between them (thin film), instability and rupture of this film. However, it is possible to reach a stable film formation with no evidence to coalescence. The rupture process takes place when the thin film thickness is less than a critical value 10-100nm. At this thickness the instability is mainly due to the long-range intermolecular forces, such as the van der Waals attractive, electrostatic repulsive and other forces. Then, if the film thickness is bigger than the critical value, it is sufficient to consider only the hydrodynamic forces due to inertia, viscosity and capillarity.

There exist different models for treating theoretically the free thin film dynamics: linear and non-linear drainage; linear and non-linear drainage and rupture. The first class of models refers to macroscopic films drainage before reaching the critical value thickness. On the other hand the drainage models consider the mobility of the interfaces, i.e., immobile, partially mobile and fully mobile interfaces. The fully mobile interfaces correspond to vanishing tangential stresses on interfaces, while for the immobile ones their tangential velocities are zero. Klaseboer et al. [3] treat experimentally and theoretically the drainage of the thin film between two deformable spherical drops approaching each other. They present two numerical models based on the lubrication assumption for both types of interface mobility. The numerical results for the film thickness and thinning rate are confirmed by their experiment for a wide range of capillarity number. The thin film is formed between the deformed drops and the typical dimple shape is also observed. A similar numerical model for drainage and rupture of thin films with partially mobile interfaces is proposed by Saboni et al. [6]. The film thickness evolution in time is obtained both in the absence and presence of van der Waals forces. For small enough film thickness the van der Waals forces become dominant and film rupture is reached, i.e., zero film thickness, at finite time. However, if van der Waals forces are not taken into account, an effective critical film rupture thickness (bigger than zero) corresponds to the same time.

The linear instabilities studies are well reviewed in [1; 4; 11]. Some of their shortcomings are discussed in [1], where an evolutionary one-dimensional system for non-linear rupture dynamics is derived at the presence of van der Waals forces. Since a long-wave asymptotics of the full Navier-Stokes equations and boundary conditions on the film interfaces is used, the film is practically infinite in the longitudinal direction. A similar model of non-linear rupture is proposed in [11] for two separate geometries: line rupture and point rupture. For both cases the one-dimensional transient system is solved numerically with periodic boundary conditions for the thickness and longitudinal velocity. Self-similar solutions of the system, becoming singular near to the rupture, are also found to be in good agreement with the numerical ones.

In [9] the free film is approached as a free liquid/solid shell-like body with variable thickness symmetric to a middle plane. The film is assumed macroscopic and van der Waals and electrostatic forces are neglected. Its interfaces are considered as fully mobile, since no surfactants are present. After aver-

aging the general balance laws along the thin film thickness (chosen as small parameter) like in the ordinary shell theory [5], the evolutionary system for the solidification of a free film of a semiconductor molten material attached to a rectangular frame surrounded by an ambient gas is derived. The liquid phase system consists of four coupled nonlinear equations for the two longitudinal velocity components, film thickness and temperature. The first three equations are similar to those used in [11]. The same 2D energy equation model for phase change of free thin films at quasi-static equilibrium is solved in [10], where different frame temperature regimes and different microgravity conditions were considered.

The goal of the present work is to analyze the dynamics of a free thin film attached to a rectangular frame surrounded by an ambient gas on the basis of the derived evolutionary system in [9]. A numerical scheme solving the 1D non-linear nonstationary system of two equations for the film thickness and longitudinal velocity is proposed. The film thickness evolution in time and longitudinal velocity are obtained for different Reynolds number and wetting angles. The steady state solution is reached asymptotically in time for  $Ca = \varepsilon$  and  $1 \leq Re \leq 100$ . For the same parameters, no film rupture is observed.

## 2. PROBLEM FORMULATION

### 2.1. General model

A planar thin liquid film attached to a rectangular rigid frame is considered. The liquid phase is supposed to be Newtonian viscous with constant density  $\rho$  and dynamic viscosity  $\mu$ . Since the film is planar, a rectangular Cartesian coordinate system  $(x, y, z)$  is chosen as a moving system. For simplicity the two free surfaces are symmetrically located with respect to the reference plane  $z = 0$  and their mean positions are  $z = \pm h/2$ , where  $h(x, y, t) = O(\varepsilon)$  and  $\varepsilon \ll 1$ . On the reference plane the symmetry conditions are imposed for the velocities  $\mathbf{v}^*(u^*, v^*, w^*)$  and pressure  $p^*$

$$u_z^* = v_z^* = w^* = p_x^* = 0 \quad \text{at} \quad z = 0$$

which imply their asymptotic expansions of the coordinate  $z = O(\varepsilon)$ :

$$\begin{aligned} (u^*, v^*, p^*) &= (u_0, v_0, p_0) + \sum_{k=1}^{\infty} z^{2k} (u_{2k}, v_{2k}, p_{2k}), \\ w^* &= zw_1 + \sum_{k=1}^{\infty} z^{2k+1} w_{2k+1}. \end{aligned} \quad (2.1)$$

Since the film flow obeys the full system of Navier-Stokes equations for  $v^*$  and  $p^*$ , the film interfaces are subjected to the kinematic boundary condition

$$h_t + u^* h_x + v^* h_y \mp 2w^* = 0 \quad \text{at} \quad z = \pm h/2, \quad (2.2)$$

that can be regarded as an equation for  $h$ .

The film interfaces are assumed fully mobile, i.e., the shear stresses on them vanish, as the ambient gas is perfect and the surface tension  $\sigma$  is constant, while the normal stress is  $\mathbf{T} \cdot \mathbf{n} \cdot \mathbf{n} = 2\sigma H$ , where  $\mathbf{T}$  stands for Cauchy stress tensor,  $\mathbf{n}$  for unit normal to interfaces and  $H$  for their mean curvature. For the planar film the latter is given by:

$$2H = \frac{[h_{xx}(4 + h_x^2) + h_{yy}(4 + h_y^2) - h_x h_y h_{xy}]}{(4 + h_x^2 + h_y^2)^{3/2}} = 0.5(h_{xx} + h_{yy}) + O(\varepsilon^3).$$

If an integration along the film thickness  $z \in [-h/2, h/2]$  is performed on (2.1), then  $u^*$ ,  $v^*$ ,  $w^*$  and  $p^*$  are asymptotic series of  $\varepsilon$  and depend on  $(x, y, t)$ . Inserting these series into (2.2), into the discussed stress conditions on the interfaces and the full Navier-Stokes equations and equating the powers of  $\varepsilon$ , a system of boundary conditions on the interfaces and governing equations is obtained. The leading order terms of  $O(\varepsilon)$  are given by:

$$h_t + (u_0 h)_x + (v_0 h)_y = 0, \quad (2.3)$$

$$\begin{aligned} \left[ \rho \frac{D u_0}{D t} - \frac{\sigma}{2} (h_{xxx} + h_{yyy}) \right] &= \frac{2\mu}{h} (2u_{0x} h + v_{0y} h)_x \\ &+ \frac{\mu}{h} (u_{0y} h + v_{0x} h)_y, \end{aligned} \quad (2.4)$$

$$\begin{aligned} \left[ \rho \frac{D v_0}{D t} - \frac{\sigma}{2} (h_{xxy} + h_{yyx}) \right] &= \frac{2\mu}{h} (2v_{0y} h + u_{0x} h)_y + \frac{\mu}{h} (v_{0x} h \\ &+ u_{0y} h)_x, \end{aligned} \quad (2.5)$$

$$p_0 = -2\mu(u_{0x} + v_{0y}) - \frac{\sigma}{2}(h_{xx} + h_{yy}). \quad (2.6)$$

The first three coupled nonlinear evolutionary equations for the longitudinal velocity components and film thickness form a closed system, while the last equation for  $p$  is solved afterwards.

The system (2.3) – (2.6) can be written in a tensor form as in [9]:

$$\frac{Dh}{Dt} = h_t + (u_0 h)_x + (v_0 h)_y = 0, \quad (2.7)$$

$$\rho \frac{D \mathbf{v}_f}{Dt} = \frac{1}{h} \operatorname{div}_s \hat{\mathbf{T}}_f, \quad (2.8)$$

where  $\mathbf{v}_f = (u_0, v_0)$  is the surface film velocity,  $\hat{\mathbf{T}}_f = -\mathbf{P}_f + \mathbf{T}_f$  is the surface film stress tensor and  $\operatorname{div}_s$  is the surface divergence. The pressure tensor (due to capillarity) is given by

$$\mathbf{P}_f = -\frac{\sigma}{2} [h \nabla_s^2 h \mathbf{I}_s + 0.5(\nabla_s h)^2 \mathbf{I}_s - \nabla_s h \otimes \nabla_s h], \quad (2.9)$$

and the film stress tensor (due to viscosity) is

$$\mathbf{T}_f = 2\mu h \left\{ (\operatorname{div}_s \mathbf{v}_f) \mathbf{I}_s + 0.5 \left[ \nabla_s \mathbf{v}_f + (\nabla_s \mathbf{v}_f)^T \right] \right\}, \quad (2.10)$$

where  $\mathbf{I}_s$  is the identical surface tensor,  $\nabla_s$  is the surface gradient and  $^T$  stands for transposition. The system (2.7), (2.8) for  $u_0$ ,  $v_0$  and  $h$  is of order  $O(\varepsilon)$ . Since the fluid is incompressible, the equation for  $w_1$  is derived from the continuity equation:

$$w_1 = -u_{0x} - v_{0y}.$$

The higher order terms of the asymptotic expansions (2.1) can be obtained in a similar way.

In the described model the gravity forces and the intermolecular forces are not considered. However, if needed, their counterparts can be added to the right hand side of (2.4), (2.5) or (2.8).

## 2.2. One dimensional model

If the frame is long enough, i.e.,  $\dim(y) \gg \dim(x) \gg \varepsilon$ , and the end effects in  $y$  direction are neglected, then the film dynamics depends only on  $(x, t)$  and the system (2.3) – (2.6) (or (2.7) – (2.10)) is simplified:

$$\frac{\partial h}{\partial t} + \frac{\partial}{\partial x}(u_0 h) = 0, \quad (2.11)$$

$$\rho \left( \frac{\partial u_0}{\partial t} + u_0 \frac{\partial u_0}{\partial x} \right) = \sigma \frac{\partial^3 h}{\partial x^3} + \frac{4\mu}{h} \frac{\partial}{\partial x} \left( h \frac{\partial u_0}{\partial x} \right). \quad (2.12)$$

Since the 1D system (2.11), (2.12) is derived from (2.7) – (2.10), its order is  $O(\varepsilon)$  ( $h = O(\varepsilon)$ ,  $u_0 = O(1)$ ,  $x = O(1)$ ). The following dimensionless variables are introduced:

$$x' = x/a, \quad t' = \mu t / \rho a^2, \quad u' = u_0 / U, \quad h' = h / \varepsilon a.$$

Then, the dimensionless form of the system (2.11) – (2.12) is given by

$$\frac{\partial h}{\partial t} + \frac{\partial}{\partial x}(uh) = 0, \quad (2.13)$$

$$\frac{\partial u}{\partial t} + Re u \frac{\partial u}{\partial x} = \frac{\varepsilon}{Ca} \frac{\partial^3 h}{\partial x^3} + \frac{4}{h} \frac{\partial}{\partial x} \left( h \frac{\partial u}{\partial x} \right), \quad (2.14)$$

where the primes are omitted (here  $x$ ,  $t$ ,  $u$  and  $h$  are dimensionless),  $Re = \rho a U / \mu$  is the Reynolds number and  $Ca = \mu U / \sigma$  the capillary number. Since the fluid dynamics is governed by the full Navier-Stokes model,  $Re > 0$ . In order to preserve the order  $O(\varepsilon)$  of (2.14), we impose the following restrictions to  $Re$  and  $Ca$ :

$$Re \geq \varepsilon, \quad Ca \leq 1.$$

If the film wets symmetrically the frame in the  $x$  direction, i.e., at  $x = \pm 1$ , then it is sufficient to consider the half line  $x \in [0, 1]$ . The boundary conditions

for  $h$  and  $u$  are the following:

$$u(0, t) = u(1, t) = 0, \quad (2.15)$$

$$\frac{\partial h}{\partial x}\Big|_{x=0} = 0, \quad \frac{\partial h}{\partial x}\Big|_{x=1} = \tan \alpha, \quad (2.16)$$

where  $\pi/2 - \alpha$  is the wetting angle. Since the liquid mass in the film is conserved during the thinning process, this condition is expressed as

$$\int_0^1 (h - h_0) dx = 0. \quad (2.17)$$

The initial conditions are given by:

$$h(x, 0) = h_0, \quad u(x, 0) = 0. \quad (2.18)$$

For simplicity in our numerical model we take  $h_0 \equiv 1$ .

As the van der Waals forces are not included in the model, the posed non-linear nonstationary problem (2.13) – (2.18) is solved till reaching a minimum value of  $h$ . It may be correspondent to a stable film shape when the process becomes steady at some finite time  $T$

$$\lim_{t \rightarrow T} h(x, t) = h(x), \quad \lim_{t \rightarrow T} u(x, t) = u(x) \quad (2.19)$$

or it may be correspondent to an effective critical film rupture thickness [6]. At this time moment  $T$  the actual film rupture occurs:

$$h(x, T) \approx 0. \quad (2.20)$$

### 3. NUMERICAL SCHEME

The finite difference scheme is constructed using the control volume method. The temporary grid  $\omega_j = j\tau$ ,  $j \geq 0$  is uniform with constant temporary step and the spatial domain  $\overline{\Omega} = [0, 1]$  is covered by equal unit grids

$$\overline{\Omega}_x = \{x_{0.5i} = (i - 1)\Delta x/2, \quad \Delta x > 0, \quad i = 1, \dots, 2N + 1; \quad x_{0.5(2N+1)} = 1\}.$$

The function  $u$  is approximated by its values in grid points with integer indexes

$$\overline{\Omega}_x^u = \{x_i = (i - 1)\Delta x, \quad i = 1, \dots, N + 1; \quad x_{N+1} = 1\},$$

while the function  $h$  – in grid points with half integer indexes

$$\overline{\Omega}_x^h = \{x_{i-0.5} = (i - 0.5)\Delta x, \quad i = 1, \dots, N + 1; \quad x_{N+1} = 1 - 0.5\Delta x\}.$$

Further, each unit of the selected grids  $\overline{\Omega_x^h}$ ,  $\overline{\Omega_x^u}$  will be connected to a control volume, whose planes pass between two adjacent units. Thus, "chess" grid is used for calculation of unknown quantities. Here for the simplicity we use notation [7].

Although the subscripts of unknown quantities are equally marked, they relate to various grid:

$$u_i = u(x_i, t_{j+1}), \quad x_i \in \overline{\Omega_x^u}, \quad h_i = h(x_i - 0.5\Delta x, t_{j+1}), \quad x_{i-0.5} \in \overline{\Omega_x^h}.$$

Two different control volumes, displaced relatively to each other by half step, are used for the two functions  $h$  and  $u$ .

Integrating (2.13) on the control volume  $[x_{i-1}, x_i]$ , we get

$$h_t + \frac{\Delta M - \Delta M_-}{\Delta x} = 0, \quad i = \overline{2, N}, \quad (3.1)$$

where  $\Delta M = \Delta M_i = \langle h \rangle_i \langle u \rangle_i$ .

The notation  $\langle \rangle$  means  $h$  and  $u$  values on cell border. Selection of these values has an important significance.

The accuracy and stability of the difference scheme depend on the approximation method. As the schemes without taking into account flow direction result in instability of calculations, we determine  $\Delta M_i$  in view of flow direction on given border. The value  $\langle u \rangle_i$  coincides with the selected grid unit system for  $u$ , for  $\langle h \rangle_i$  there is a necessity definition of function  $h$  in grid points which are not appropriate to their positions on grid pattern. In this case simple "transfer" of function values according to the coefficient sign determining convective transfer is used. As a result,

$$\Delta M_i = u_i^+ h_i + u_i^- h_{i+1},$$

where

$$u_i = u_i^+ + u_i^-, \quad u_i^+ = 0.5(u_i + |u_i|) \geq 0, \quad u_i^- = 0.5(u_i - |u_i|) \leq 0.$$

Then in accordance with conditions (2.15)

$$\Delta M_1 = 0, \quad \Delta M_N = 0.$$

The system (3.1) is described by  $N - 1$  equations corresponding to the unknowns  $h_i$ ,  $i = \overline{2, N - 1}$ . The values  $h(x_1, t_{j+1})$  and  $h(x_N, t_{j+1})$  are still unknown and will be determined from the boundary conditions (2.15).

A similar differential analogue for the motion equation is obtained after integrating the equation (2.14) in the control volume  $[x_{i-0.5}, x_{i+0.5}]$ :

$$u_{\bar{i}} + Re(\bar{u}^- u_x + \bar{u}^+ u_{\bar{x}}) = \frac{\varepsilon}{Ca} h_{\bar{x}x\bar{x}} + \frac{4}{\bar{h}} (hu_{\bar{x}})_x, \quad i = \overline{2, N - 1}, \quad (3.2)$$

$$u_1 = 0, \quad u_N = 0,$$

where  $\bar{h} = 0.5(h_i + h_{i+1})$ ,

$$h_{\bar{x}x\dot{x}} = \begin{cases} h_{\bar{x}x\dot{x}} & \text{for } i = \overline{3, N-2}; \\ (h_4 - 3h_3 + 2h_2)/\Delta x^3 & \text{for } i = 2; \\ (\tan \alpha \Delta x - 2h_N + 3h_{N-1} - h_{N-2})/\Delta x^3 & \text{for } i = N-1; \end{cases}$$

The scheme (3.1) – (3.2) approximates the differential equations with the error  $O(\Delta x + \Delta t)$ . The analysis of stability is carried out by using the differential approximation mechanism [8], the stability depends on the sign of diffusion coefficient of appropriate differential approximation.

When constructing the differential scheme inside the integration area the weight (mass) and momentum are preserved. For example, for (3.1) the mass preservation law gives the condition (2.17).

The system (3.1) – (3.2) is nonlinear. For its solution the following iterative process is proposed:

$$h_t^{s+1} + (\Delta M^s - \Delta M_-^s)/\Delta x = 0, \quad x_i \in \overline{\Omega_x^h}, \quad (3.3)$$

$$u_{\bar{t}}^{s+1} + Re(\bar{u}^{-s} u_x^{s+1} + \bar{u}^{+s} u_{\bar{x}}^{s+1}) = \frac{\varepsilon}{Ca} h_{\bar{x}x\dot{x}}^{s+1} + \frac{4}{\bar{h}^{s+1}} (h^{s+1} u_{\bar{x}}^{s+1})_x, \\ x_i \in \overline{\Omega_x^u}, \quad (3.4)$$

The use of velocities from previous time layer makes the iterative process unstable. Therefore the following order of calculations is used. The problem is solved in steps: first we find  $h^{s+1}$  from the system (3.3), and then we solve system (3.4) for  $u^{s+1}$  by the elimination method. As iteration ending conditions the errors estimates are imposed:

$$|u_i^{s+1} - u_i^s| \leq \varepsilon_u \quad \text{or} \quad |(u_i^{s+1} - u_i^s)/u_i^s| \leq \varepsilon_u, \\ |h_i^{s+1} - h_i^s| \leq \varepsilon_h \quad \text{or} \quad |(h_i^{s+1} - h_i^s)/h_i^s| \leq \varepsilon_h,$$

where  $\varepsilon_u$  and  $\varepsilon_h$  are given constants determining accuracy of the iterative process.

The problem is recurrently solved on temporary layers  $t_j = t_{j-1} + \Delta t$ ,  $j = \overline{1, J}$ , until one of conditions (2.19) or (2.20) is fulfilled. For the numerical process the first condition is given as  $|h_i - h_{ij}| \leq \varepsilon_{min}$ , when the process becomes asymptotically steady at finite time  $T = t_j$ , with  $j = J$  and  $\varepsilon_{min}$  is a given number. The second condition reads as  $h_{ij} = O(\Delta x)$ .

#### 4. RESULTS AND DISCUSSION

If  $Ca \rightarrow 0$ , the steady state solution of the problem (2.13) – (2.17) can be achieved independently on  $Re$ . It is given by the analytical formulas:

$$h(x) = 0.5(x^2 - 1/3) \tan \alpha + 1, \quad u(x) \equiv 0. \quad (4.1)$$



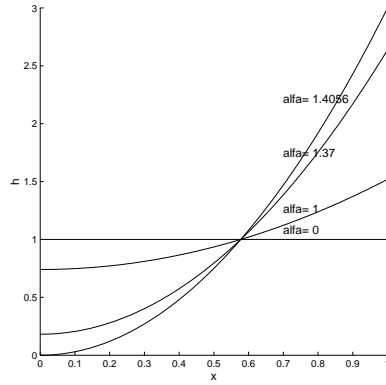


**Figure 1.** Analytical solution of  $h(x)$  for different  $\alpha$ .

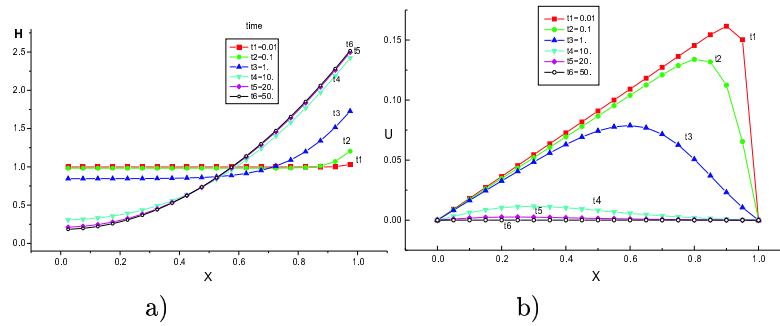


**Figure 2.** Evolution in time of  $h(x)$ ,  $u(x)$  of stationary problem for  $Ca = 0.15\epsilon$ ,  $\alpha = 1, 37$ .

The minimum value of  $h(x)$  is reached at  $x = 0$  and it depends on the angle  $\alpha$ . Then  $h(x) > 0$  for  $\alpha \leq 1.40564$  and its graphs are shown in Fig.1. The negative values of  $h$ , i.e.,  $h(0) \leq 0$  for  $\pi/2 > \alpha > 1.40564$ , are not solutions of our physical problem of thin film dynamics. Further in the numerical experiments, we have obtained the steady state solution (4.1) for different times  $T$ , according to the condition (2.19).

The numerical solution of the steady state problem for  $Ca = 0.15\epsilon$ ,  $\alpha = 1.37$  with initial conditions  $u(x) \equiv 0$  and  $h(x) \equiv 1$  is presented in Fig.2. As it can be seen from Fig.2a the velocity quickly increases at the initial moment  $t_1$ . Then the velocity decreases; at  $t_6$  it is equal to zero, when the solution has reached its steady state. The final solution  $h$  at  $t_6 = 50$  (see Fig.2b) is validated by the exact steady state solution (4.1) represented in Fig.1 for  $\alpha = 1.37$ . The integral mass conservation (2.17) is preserved with the order  $3 \times 10^{-6}$ .

The presented numerical scheme has been applied for  $Ca = \epsilon$ ,  $\alpha < 1.40564$  and large range of  $Re$ . The grid steps for all calculations are  $\Delta x = 0.02$ ,

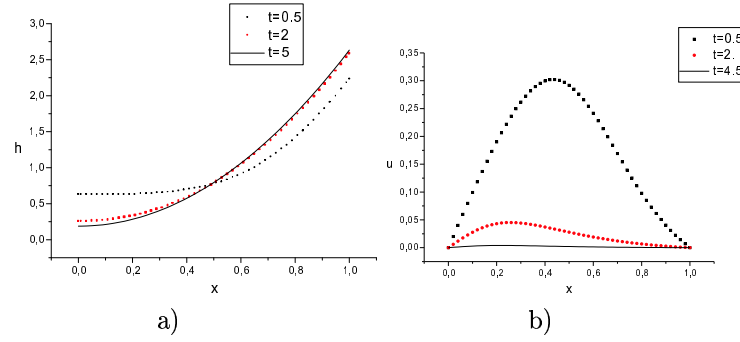


**Figure 3.** Evolution in time of  $h(x)$ ,  $u(x)$  for  $Re = 10$ ,  $Ca = \varepsilon$ ,  $\alpha = 1, 37$ .

$$\Delta t = 1.e^{-4}.$$

In Fig.3 and Fig.4,5 the film thickness  $h$  and longitudinal velocity  $u$  distributions in space and time are presented for  $Re = 10$  and  $Re = 100$ , respectively. For both cases  $\alpha = 1.37$  and the film rupture does not occur. The solution reaches its steady form, but for different times:  $T = 5$  for  $Re = 10$  and  $T = 4.6$  for  $Re = 100$ . The other numerical experiments with smaller  $Re$  confirm this tendency, that the time  $T$  increases with the decrease of  $Re$ . The condition (2.19) is fulfilled with the accuracy  $O(\Delta x)$  for  $h$  and  $O(10^{-5})$  for  $u$ .

Analyzing Fig.4 and Fig.5, we see that at times smaller than  $T$ , the film shape for  $Re = 100$  is convex at the center ( $x = 0$ ), i.e., a dimple is formed.

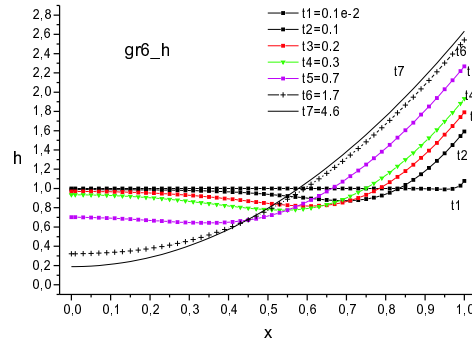


**Figure 4.** Evolution in time of  $h(x)$  for  $Re = 100$ ,  $Ca = \varepsilon$ ,  $\alpha = 1, 37$ .

## 5. CONCLUSIONS

In the present work we study the dynamics of a free thin film attached to the rectangular frame surrounded by an ambient gas. The considered model is derived in [9]. The 1D problem consisting of a non-linear unstationary system of two equations for the film thickness and longitudinal velocity is posed. For

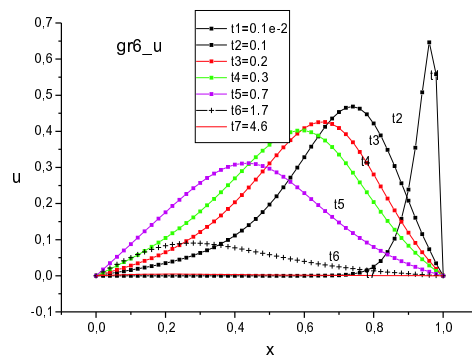


**Figure 5.** Evolution in time of  $u(x)$  for  $Re = 100$ ,  $Ca = \varepsilon$ ,  $\alpha = 1, 37$ .

solving it a finite difference numerical scheme with "chess" grid pattern is proposed. Since the system is non-linear, in order to linearize it, an iterative procedure is constructed.

The film thickness evolution in time and longitudinal velocity are obtained for different  $Re$ . The steady state solution is reached asymptotically in time for  $Ca = \varepsilon$  and  $1 \leq Re \leq 100$ . For the same parameters, no film rupture is observed.

A parametrical analysis of film dynamics in the absence and in the presence of van der Waals forces in the model will be a subject of future studies. An appropriate numerical scheme will be developed for the 2D model.

## REFERENCES

- [1] T. Erneux and S.H. Davis. Nonlinear rupture of free films. *Phys. Fluids*, **A 5**(5), 1117 – 1122, 1993.
- [2] I.B. Ivanov and D.S. Dimitrov. Thin film drainage. In: *Thin liquid films. Fundamentals and applications*. New York and Basel, 1988.
- [3] E. Klaseboer, J.Ph. Chevaillier, C. Gourdon and O. Masbernat. Film drainage between colliding drops at constant approach velocity: experiments and modeling. *J. Colloid Interface Sci.*, **229**, 2000.
- [4] C. Maldarelli and R.K. Jain. The hydrodynamic stability of thin films. In: *Thin liquid films. Fundamentals and applications*. New York and Basel, 1988.
- [5] P.M. Naghdi. The theory of shells and plates. In: *Handbuch der Physik*, volume VI a/2, Springer Verlag - Heidelberg, New York, 1974.
- [6] A. Saboni, C. Gourdon and A.K. Chesters. Drainage and rupture of partially mobile films during coalescence in liquid-liquid systems under a constant interaction force. *J. Colloid Interface Sci.*, **175**, 27 – 35, 1995.
- [7] A. Samarskii. *Theory of difference schemes*. Nauka, Moscou, 1989.
- [8] Yu.I. Shokin and N.N. Yanenko. *Method differential approximation*. Nauka, Novosibirsk, 1985.
- [9] S. Tabakova. Solidification of free thin films. *Theoretical and Applied Mechanics*, **30**(2), 39 – 49, 2000.

- [10] S. Tabakova and L. Carotenuto. Numerical modeling of the solidification of free thin films. *Microgravity Quarterly*, **4**(1), 55 – 61, 1994.
- [11] D. Vaynblat, J.R. Lister and T.P. Witelski. Rupture of thin viscous films by van der Waals forces: Evolution and self-similarity. *Phys. Fluids*, **13**(5), 1130 – 1140, 2001.

### **Laisvosios plonosios plėvelės dinamikos skaitinis modeliavimas**

L. Popova, G. Gromyko, S. Tabakova

Nagrinėjamas svarbus dujų dinamikai plonosios plėvelės judėjimo matematinio modeliavimo uždavinys. Atliktą diferencialinių lygčių asimptotinę analizę. Pasiūlyta skirtuminė schema skaičiavimams atlikti ir pateikti skaitinių eksperimentų rezultatai.